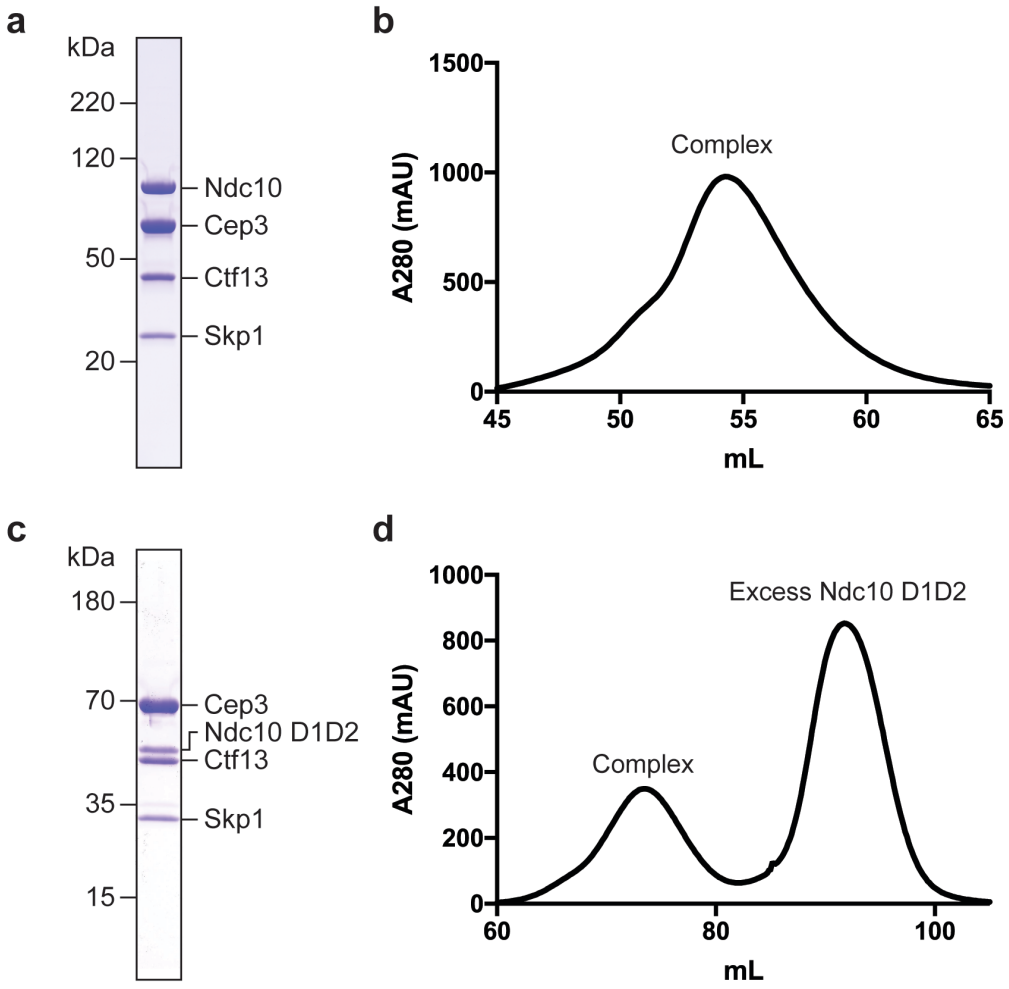

Figure S1. Purification of *in-vitro* reconstituted CBF3 core complexed with full-length Ndc10 or monomeric Ndc10 D1D2. (a) SDS-PAGE analysis of CBF3-Ndc10 complex. (b) Size-exclusion chromatogram for full-length complex. (c) SDS-PAGE analysis of uncrosslinked CBF3-Ndc10 D1D2. (d) Size-exclusion chromatogram for uncrosslinked CBF3-Ndc10 D1D2 complex.

6946 micrographs (1,653,364 particles)

Iterative 2D classification

753,528 particles

3D Classification

Select best class for 3D auto-refinement (367,572 particles, 48.8%)

Relion Bayesian Polishing

Signal Subtraction (Ndc10 D2) and Masked Classification

Select best class for 3D auto-refinement (227,684 particles, 30.2%)

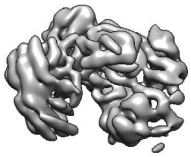

CTF Refinement

Focused classification without alignment on Cep3b, Ctf13, Skp1, and Ndc10 D1

Focused classification without alignment on CBF3 Core

Select best class for 3D auto-refinement (130,143 particles, 17.3%)

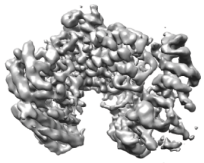

CBF3 core
Resolution: 4.0Å

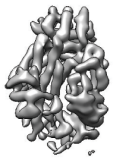

Select **best** class for 3D auto-refinement (63,177 particles, 8.4%)

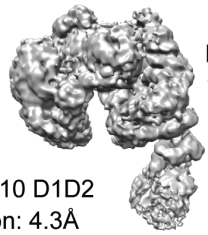

CBF3-Ndc10 D1D2
Resolution: 4.3Å

Restore Ndc10 D2 Signal

3D auto-refinement

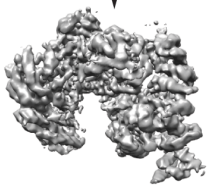

CBF3-Ndc10 D1
Resolution: 4.1Å

Figure S2. Data processing and model refinement pipeline. Particles of crosslinked CBF3-Ndc10 D1 were picked from cryo-EM micrographs collected over two sessions (Table 1). After iterative 2D classification, 3D classification was performed on the remaining particles, followed by 3D auto-refinement on the best class. After Bayesian polishing in RELION-3, signal for Ndc10 D2 was subtracted in real-space and masked classification was performed. Particles belonging to the best class were selected and used for per-particle CTF refinement, followed by a further round of 3D auto-refinement, with the updated CTF parameters. Two separate analysis strategies yielded density maps of CBF3 core and CBF3-Ndc10 D1D2. Focused classification without alignment of CBF3 core, followed by 3D auto-refinement, produced a map of CBF3 core with 4.0 Å resolution, and focused classification without alignment on Cep3b, Ctf13, Skp1, and Ndc10 D1, followed by selection of the class with clear Ndc10 D1 density and 3D auto-refinement produced a map of CBF3-Ndc10 D1 with 4.1 Å resolution. From the CBF3-Ndc10 D1 map, restoration of Ndc10 D2 signal and 3D auto-refinement produced the CBF3-Ndc10 D1D2 map with 4.3 Å resolution.

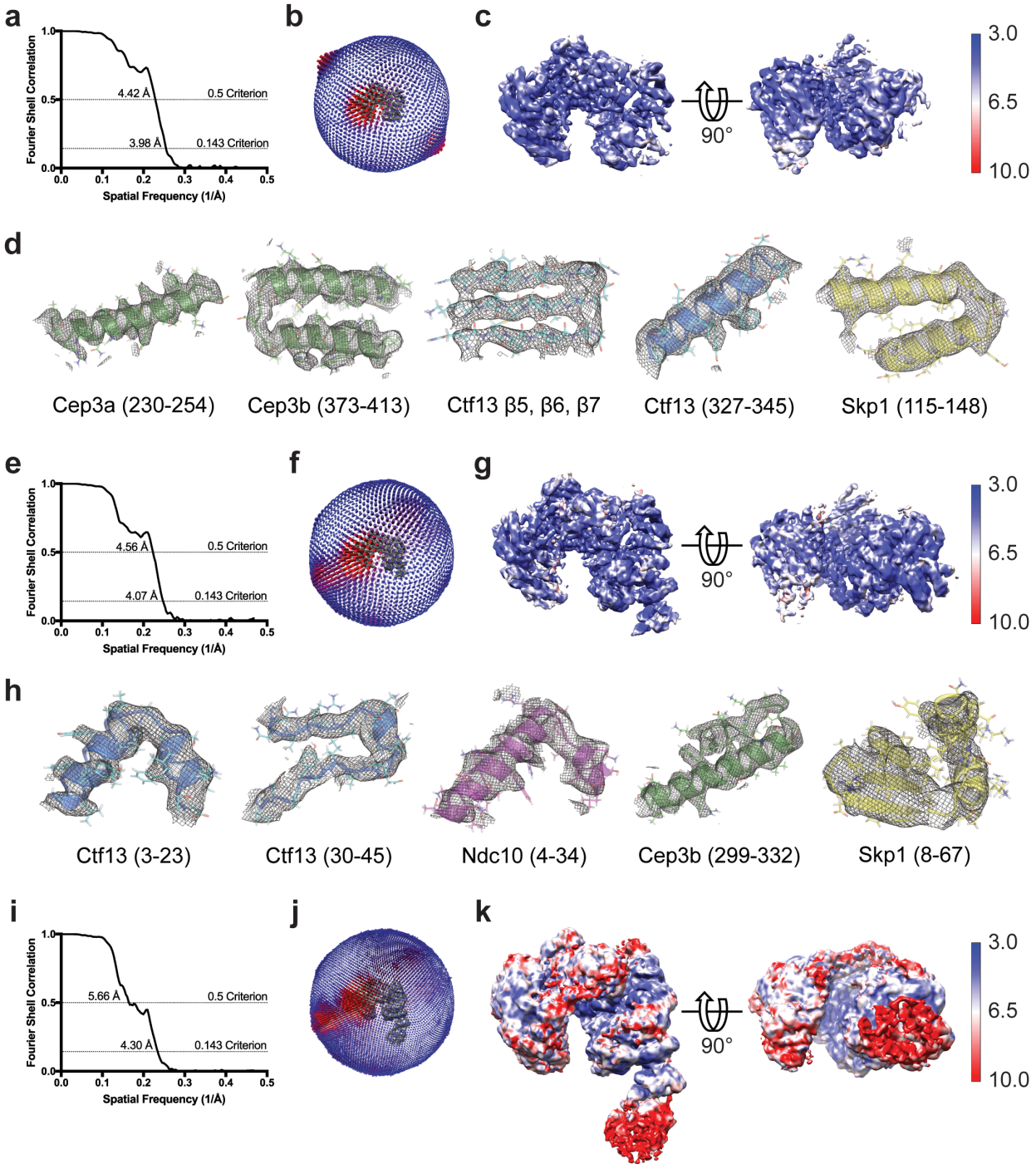

Figure S3. Details of density maps from cryo-EM analysis. (a) Fourier shell correlation between half maps of CBF3 core. (b) Angular distribution of particles in CBF3 core map. (c) Local resolution estimates of CBF3 core map. (d) Examples of molecular model built into final density map for CBF3 core. (e) Fourier shell correlation between half maps of CBF3-Ndc10 D1. (f) Angular

distribution of particles in CBF3-Ndc10 D1 map. (g) Local resolution estimates of CBF3-Ndc10 D1 map. (h) Examples of molecular model built into final density map for CBF3 core including elements of the Ctf13-Ndc10 interface (Ctf13 residues 30-45 and Ndc10 residues 4-34). (i) Fourier shell correlation between half maps of CBF3-Ndc10 D1D2. (j) Angular distribution of particles in CBF3-Ndc10 D1D2 map. (k) Local resolution estimates of CBF3-Ndc10 D1D2 map.

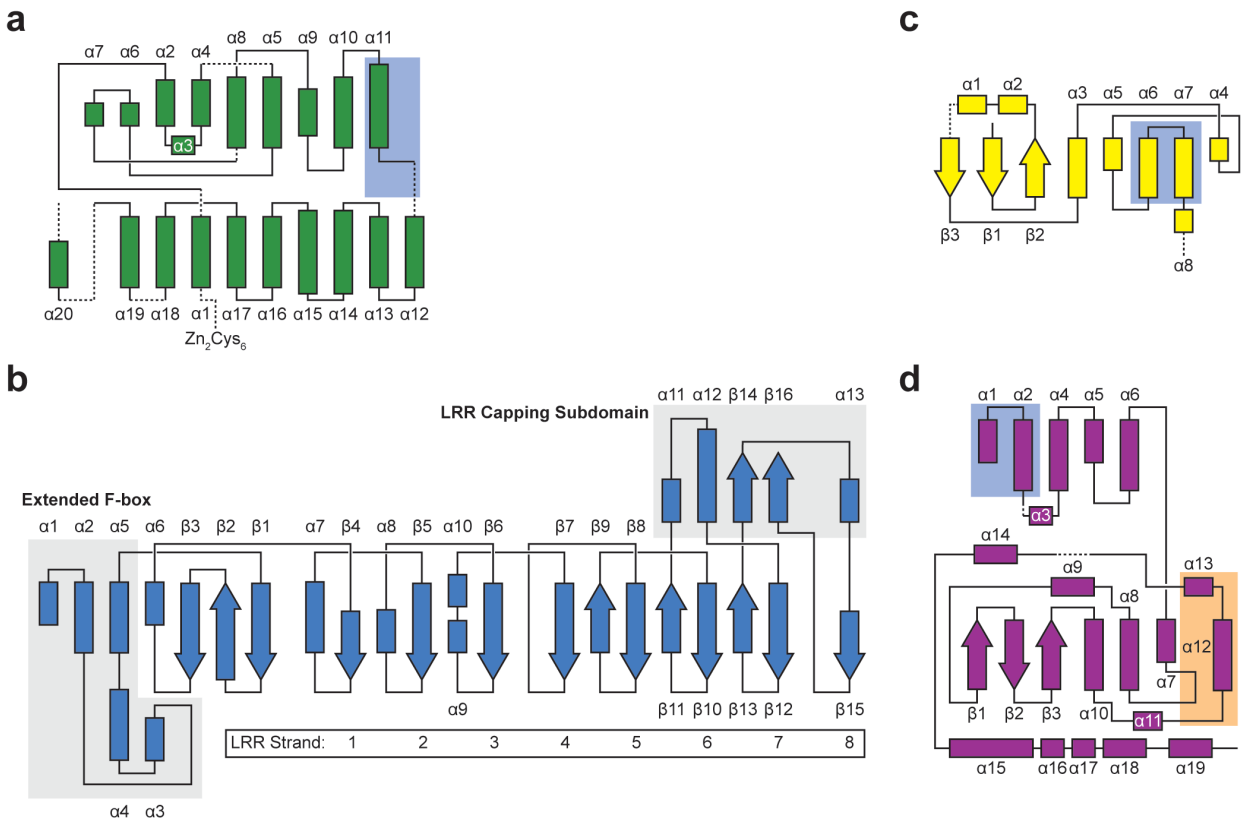

Figure S4. Secondary structure diagrams for CBF3-Ndc10 D1D2 complex. (a) Secondary structure diagram for Cep3a and Cep3b. Region of the Cep3b that interacts with Ctf13 is boxed in blue. (b) Secondary structure diagram for Ctf13. The extended F-box and the LRR capping subdomain are boxed in gray. (c) Secondary structure diagram for Skp1. Region of Skp1 that interacts with Ctf13 is boxed in blue. (d) Secondary structure diagram for Ndc10 D1D2. Region of Ndc10 that interacts with Ctf13 is boxed in blue. DNA binding interface is boxed in orange.

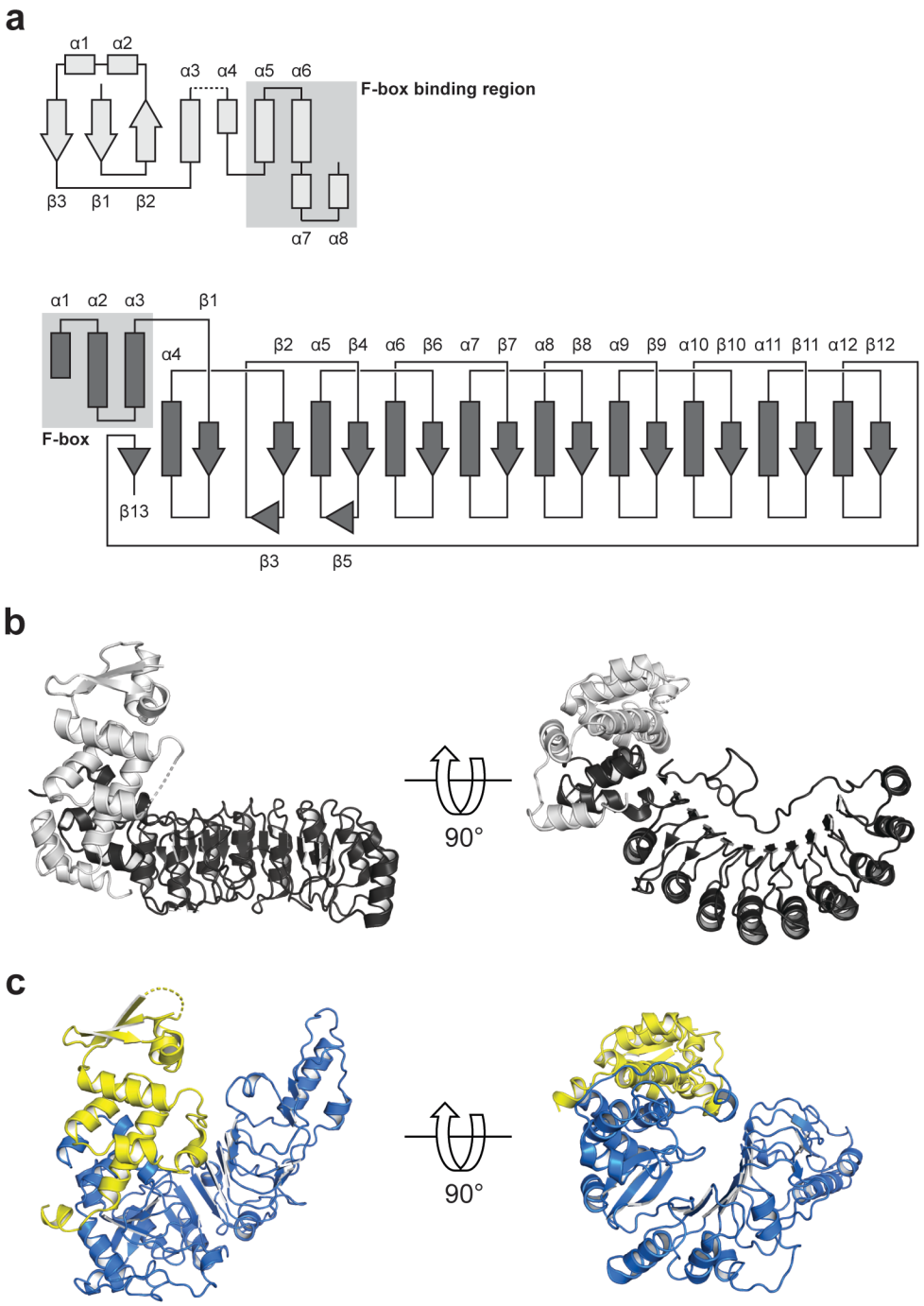

Figure S5. Comparison of human Skp1-Skp2 and *K. lactis* Skp1-Ctf13. (a) Secondary structure diagrams of Skp1 and Skp2 (PDB 1FQV). (b) Crystal structure of Skp1-Skp2 in two orientations. (c) Model of *K. lactis* Skp1-Ctf13 in two orientations.

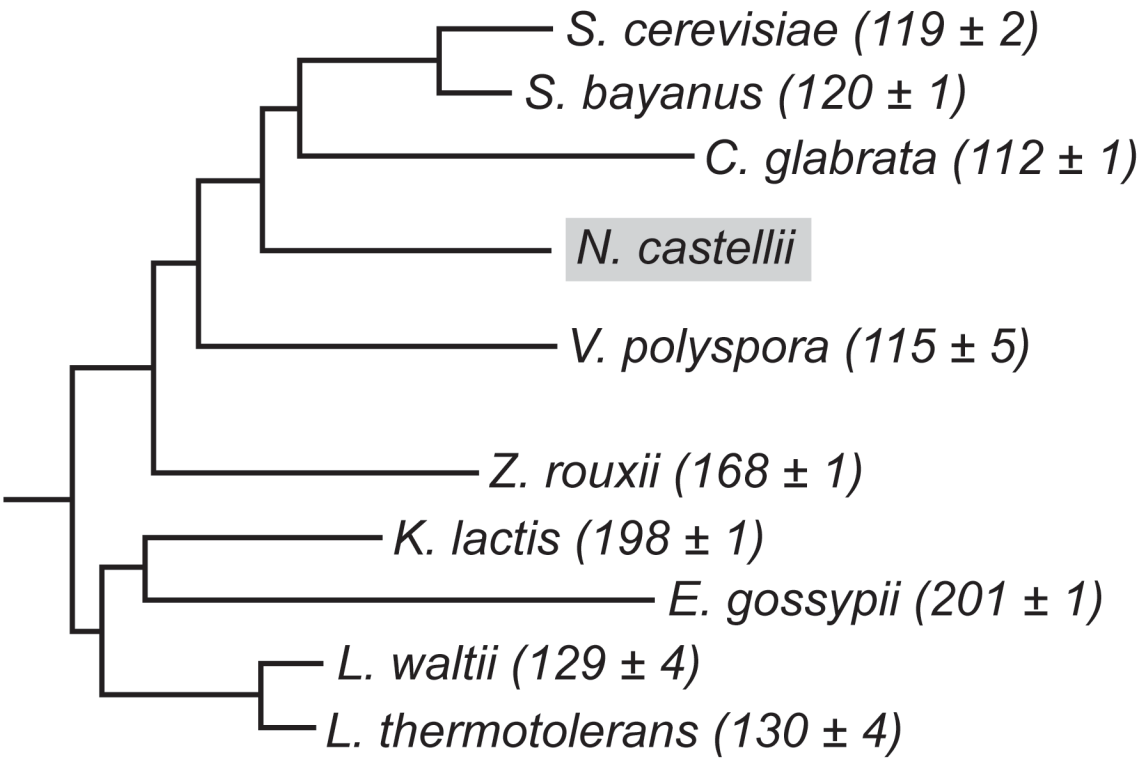

Figure S6. (a) Phylogenetic tree of budding yeast. Phylogeny was generated from [32] based on data from [33]. Centromere lengths and standard deviation among all chromosomes is shown in parenthesis. Centromere sequences obtained from [14]. *N. castelli* has an unconventional point centromere with a discontinuous CDEII. It is boxed in gray to indicate this difference. Scale bar is 0.01 substitutions/site.